

# Structure Aware Negative Sampling in Knowledge Graphs

Kian Ahrabian<sup>\*,1,3</sup>, Aarash Feizi<sup>\*,1,3</sup>, Yasmin Salehi<sup>\*,2</sup>,  
William L. Hamilton<sup>1,3,4</sup> and Avishek Joey Bose<sup>1,3</sup>

<sup>1</sup> School of Computer Science, McGill University, Canada

<sup>2</sup> Department of Electrical and Computer Engineering, McGill University, Canada

<sup>3</sup> Montreal Institute of Learning Algorithms (Mila), Canada

<sup>4</sup> Canada CIFAR AI Chair

{kian.ahrabian, aarash.feizi, yasmin.salehi }  
{@mail.mcgill.ca }

## Abstract

Learning low-dimensional representations for entities and relations in knowledge graphs using contrastive estimation represents a scalable and effective method for inferring connectivity patterns. A crucial aspect of contrastive learning approaches is the choice of corruption distribution that generates hard negative samples, which force the embedding model to learn discriminative representations and find critical characteristics of observed data. While earlier methods either employ too simple corruption distributions, i.e. uniform, yielding easy uninformative negatives or sophisticated adversarial distributions with challenging optimization schemes, they do not explicitly incorporate known graph structure resulting in suboptimal negatives. In this paper, we propose Structure Aware Negative Sampling (SANS), an inexpensive negative sampling strategy that utilizes the rich graph structure by selecting negative samples from a node’s  $k$ -hop neighborhood. Empirically, we demonstrate that SANS finds semantically meaningful negatives and is competitive with SOTA approaches while requires no additional parameters nor difficult adversarial optimization.

## 1 Introduction

Knowledge Graphs (KGs) are repositories of information organized as factual triples  $(h, r, t)$ , where head and tail entities are connected via a particular relation  $(r)$ . Indeed, KGs have seen wide application in a variety of domains such as question answering (Yao and Van Durme, 2014; Hao et al., 2017; Moldovan and Rus, 2001) and machine reading (Weissenborn et al., 2018; Yang and Mitchell, 2017) to name a few and have a rich history within the natural language processing (NLP) community (Berant et al., 2013; Yu and Dredze, 2014; Collobert and Weston, 2008; Peters et al., 2019). While

often large, real-world KGs such as FreeBase (Bollacker et al., 2008) and WordNet (Miller, 1995) are known to be incomplete. Consequently, KG completion via link prediction constitutes a fundamental research topic ameliorating the practice of important NLP tasks (Sun et al., 2019; Angeli and Manning, 2013).

In recent years, there has been a surge of methods employing graph embedding techniques that encode KGs into a lower-dimensional vector space facilitating easier data manipulation (Zhang et al., 2019) while being an attractive framework for handling data sparsity and incompleteness (Wang et al., 2018). To learn such embeddings, contrastive learning has emerged as the de facto gold standard. Indeed, contrastive learning approaches enjoy significant computational benefits over methods that require computing an exact softmax over a large candidate set, such as over all possible tail entities given a head and relation. Another important consideration is modeling needs, as certain assumptions are best expressed as some score or energy in margin-based or un-normalized probability models (Smith and Eisner, 2005). For example, modeling entity relations as translations or rotations in a vector space naturally leads to a distance-based score to be minimized for observed entity-relation-entity triplets (Bordes et al., 2013).

Leveraging contrastive estimation to train KG embedding models involves optimizing the model by pushing up the energy with respect to observed positive triplets while simultaneously pushing down energy on negative triplets. Consequently, the choice of negative sampling distribution plays a crucial role in shaping the energy landscape as simple random sampling—e.g. Noise Contrastive Estimation (NCE) (Gutmann and Hyvärinen, 2010)—produces negatives that are easily classified and provide little information alongside in the form of a gradient signal. This is easily remedied if the

\*Equal contribution, names ordered alphabetically.

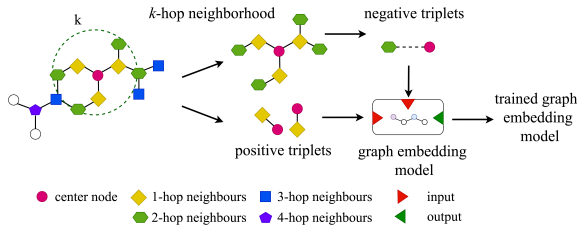


Figure 1: Our proposed approach for training a graph embedding model. In this illustration,  $k$  is set to 2.

corruption process selects a hard negative example through more complex negative sampling distribution, such as adversarial samplers (Cai and Wang, 2018; Bose et al., 2018; Sun et al., 2019). However, adversarial negative sampling methods are computationally expensive, while more tractable approaches—e.g. cache-based methods (Zhang et al., 2019)—are not tailored to the KG setting as they fail to incorporate known graph structure as part of the sampling process. This raises the important question of whether we can obtain a computationally inexpensive negative sampling strategy while benefiting from the rich graph structure of KGs.

**Present Work.** In this work, we introduce *Structure Aware Negative Sampling* (SANS), an algorithm that utilizes the graph structure of a KG to find hard negative examples. Specifically, SANS constructs negative samples using a subset of entities restricted to either the head or tail entity’s  $k$ -hop neighborhood. We hypothesize that entities that are within each other’s neighborhood but share no direct relation have higher chances of being related to one another and thus are good candidates for negative sampling. We also experiment with a dynamic sampling scheme based on random walks to approximate a node’s local neighborhood. Empirically, we find that negative sampling using SANS consistently leads to improvements upon uniform sampling and sophisticated Generative Adversarial Network (Goodfellow et al., 2014) (GAN) based approaches at a fraction of the computational cost, and is competitive with other SOTA approaches with no added parameters.

## 2 Related Work

**Negative Sampling.** Negative sampling is a method that can be employed to enable the scaling of log-linear models. In essence, negative sampling resolves computational intractability of computing the normalization constant by changing the task to

distinguishing observed positive data and fictitious negative examples that are generated by corrupting the positive examples. This general approach is a simplification of NCE, which is based on a Monte-Carlo approximation of the partition function used in Importance Sampling (IS) (Bengio et al., 2003). **Non-Fixed Negative Sampling.** As proposed in (Mikolov et al., 2013), negative triplets can be generated using a uniform sampling scheme. However, such uniform and fixed sampling schemes result in easily-classified negative triplets during training, which do not provide any meaningful information (Sun et al., 2019; Zhang et al., 2019). Hence, as the training progresses, most of the sampled negative triplets receive small scores and almost zero gradients, impeding the training of the graph embedding model after only a small number of iterations.

To address the issue of easy negatives, Sun et al. (2019) propose Self-Adversarial negative sampling, which weighs each sampled negative according to its probability under the embedding model. Alternatively, the authors in (Wang et al., 2018) and (Cai and Wang, 2018) try creating high-quality negative samples by exploiting GANs, which, while effective, are expensive to train and require black-box gradient estimation techniques. Another elegant approach that uses fewer parameters and is easier to train compared to GAN-based methods is NSCaching (Zhang et al., 2019), which involves using a cache of high-quality negative triplets—i.e. those with high scores.

## 3 Structure Aware Negative Sampling

Given an observed positive triplet  $(h, r, t)$ , a negative sample can be constructed by corrupting either the head or tail entity to form a new triplet—i.e.  $(h', r, t')$ —where either  $h', t' \in E$ , where  $E$  is the set of all entities in the KG. Additionally, we assume that the graph embedding models are trained using a loss function of the following form:

$$\mathcal{L} = -\log \sigma(\gamma - d_r(\mathbf{h}, \mathbf{t})) - \sum_{i=1}^n \frac{1}{n} \log \sigma(d_r(\mathbf{h}'_i, \mathbf{t}'_i) - \gamma) \quad (1)$$

where  $d_r(h, t)$  denotes the score assigned to the compatibility of head and tail entities under the relation  $r$ ,  $\gamma$  is a fixed margin,  $\sigma$  is the sigmoid function, and  $n$  is the number of negative samples.

In this paper, we seek to explicitly use the rich graph structure surrounding a particular node when

generating negative triplets. We motivate our approach based on the observation that prior work in learning word embeddings (Mikolov et al., 2013), where negative sampling has historically developed, lacked the richness of graph structure that is immediately accessible in the KG setting. Consequently, we hypothesize that enriching the negative sampling process with structural information can yield harder negative examples, crucial to learning effective embeddings. Fig. 1 highlights our approach, which requires the construction of the  $k$ -hop neighborhood ( $\mathbb{K}$ ) for each node at its first step,

$$\mathbb{K} = S^+(A^k + A^{k-1}) \quad (2)$$

for  $k > 0$ , where  $k$  is an integer, representing the neighborhood radius,  $A$  is the KG’s adjacency matrix, and  $S^+$  is the element-wise sign function set to 1 if a path exists and 0 otherwise.

To construct negatives triplets, we may now simply sample from the nonzero cell of  $\mathbb{K}$ , which represents a subset of all entities for each node in the KG—i.e.  $\mathbb{K} \subset \mathbf{1}^{E \times E}$ . Intuitively, SANS exploits the locality of an entity’s neighborhood, where negative samples are defined as entities that are not directly linked under a relation  $r$  but can be accessed through a path of at most length  $k$ . We argue that such local negatives are harder to distinguish and lead to higher scores as evaluated by the embedding model. One important technical detail in constructing  $\mathbb{K}$  is the existence of multiple relation types, which requires an additional dimension to represent the graph connectivity as adjacency and  $k$ -hop tensors.

### 3.1 Variants of SANS

Although SANS requires a one-time preprocessing step to construct  $\mathbb{K}$  as defined in Eqn. 2, this may still be costly for large and dense KGs. To combat this inefficiency, we introduce *RW-SANS* in Alg. 1, which uses  $\omega$  random walks (Perozzi et al., 2014) of length  $k$  in the adjacency tensor to approximate the  $k$ -hop neighborhood.

As SANS constructs a local neighborhood from which negative samples are drawn, it can also be combined with other negative sampling approaches. In this work, we extend the Self-Adversarial approach in (Sun et al., 2019) and combine it with SANS by restricting the negative triplet candidate set to the  $k$ -hop neighborhood. In the subsequent sections, we refer to this technique as *Self-Adversarial (Self-Adv.) SANS*, whereas the former approach is referred to as *Uniform SANS*.

---

#### Algorithm 1 Approximating the $k$ -hop Neighborhood Using Random Walks

---

**Input:**  $A, R, k, \omega \{A\}$ : adjacency tensor,  $R$ : set of relation types,  $k$ : # of  $k$ -hops,  $\omega$ : # of random walks  
 $K \leftarrow \text{sparseTensor}(|A| \times |R| \times |A|)$   
**for all** entity  $e$  **do**  
     $K[e] \leftarrow \text{randomWalk}(k, \omega)$   
**end for**  
**return**  $K$

---

## 4 Experiments

We investigate the application of SANS-based negatives to train KG embedding models based on the TransE, DistMult, and RotatE models for the task of KG completion\*. We evaluate our proposed approach on standard benchmarks, consisting of FB15K-237 (Bollacker et al., 2008), WN18 and WN18RR (Miller, 1995). From our experiments we seek to answer the following questions:

- (Q1) **Hard Negatives: Can we sample hard negatives purely using graph structure?**
- (Q2) **Can we combine graph structure with other SOTA negative samplers?**
- (Q3) **Can we effectively approximate the adjacency tensor with random walks?**

In our experiments, we rely on three representative baselines, namely uniform negative sampling (Bordes et al., 2013), KBGAN (Cai and Wang, 2018), and NSCaching (Zhang et al., 2019). We also compare with the current SOTA approach in Self-Adversarial negative sampling (Sun et al., 2019), and we test whether local graph structure can also be leveraged in this setting.

### 4.1 Results

We now address the core experimental questions.

**Q1:** Table 1 summarizes our main quantitative results where we highlight SANS and RW-SANS. We also compute the difference between the best variant of SANS against the best performing baseline in row  $\Delta$ . Overall, we find that SANS negatives almost always lead to harder negative samples over Uniform and KBGAN negatives on all three datasets. Furthermore, SANS achieves competitive performance with NSCaching when combined

---

\*Code available at <https://github.com/kahrabian/SANS>

Score Function	Algorithm	FB15K-237		WN18		WN18RR	
		Hit@10 (%)	MRR	Hit@10 (%)	MRR	Hit@10 (%)	MRR
TransE	KBGAN (Cai and Wang, 2018)	46.59	0.2926	94.80	0.6606	43.24	0.1808
	NSCaching (Zhang et al., 2019)	47.64	<b>0.2993</b>	94.63	<b>0.7818</b>	47.83	0.2002
	Uniform (Sun et al., 2019)	<b>48.03</b>	0.2927	<b>95.53</b>	0.6085	<b>49.63</b>	<b>0.2022</b>
	Uniform SANS (ours)	48.35	0.2962	95.09	<b>0.8228*</b>	51.15	0.2254
	Uniform RW-SANS (ours)	<b>48.50*</b>	<b>0.2981*</b>	<b>95.22*</b>	0.8195	<b>53.41*</b>	<b>0.2317*</b>
	$\Delta$	+0.47	-0.0012	-0.31	+0.0410	+3.78	+0.0295
DistMult	KBGAN	39.91	0.2272	93.08	0.7275	29.52	0.2039
	NSCaching	<b>45.56</b>	<b>0.2834</b>	<b>93.74</b>	<b>0.8306</b>	45.45	<b>0.4128</b>
	Uniform	40.26	0.2537	81.39	0.4689	<b>52.86</b>	0.3938
	Uniform SANS (ours)	41.00	0.2595	<b>93.19*</b>	<b>0.7553*</b>	44.74	0.4025
	Uniform RW-SANS (ours)	<b>41.46*</b>	<b>0.2621*</b>	89.80	0.6235	<b>49.09*</b>	<b>0.4071*</b>
	$\Delta$	-4.10	-0.0213	-0.55	-0.0753	-3.77	-0.0057
RotatE	Uniform	<b>47.85</b>	<b>0.2946</b>	<b>96.09</b>	<b>0.9474</b>	<b>56.51</b>	<b>0.4711</b>
	Uniform SANS (ours)	48.22	0.2985	95.97	<b>0.9499*</b>	55.76	0.4769
	Uniform RW-SANS (ours)	<b>48.47*</b>	<b>0.3003*</b>	<b>96.07*</b>	0.9489	<b>57.12*</b>	<b>0.4796*</b>
	$\Delta$	+0.62	+0.0057	-0.02	+0.0025	+0.61	+0.0085

Table 1: Comparison of different negative sampling algorithms. **Bold** and **marked bold\*** numbers represent the best SOTA and SANS algorithms respectively.

Score Function	Algorithm	FB15K-237		WN18		WN18RR	
		Hit@10 (%)	MRR	Hit@10 (%)	MRR	Hit@10 (%)	MRR
TransE	Self-Adv. (Sun et al., 2019)	<b>52.73</b>	<b>0.3296</b>	<b>92.02</b>	<b>0.7722</b>	<b>52.78</b>	<b>0.2232</b>
	Self-Adv. SANS (ours)	<b>52.03*</b>	<b>0.3265*</b>	84.06	0.7136	53.21	0.2249
	Self-Adv. RW-SANS (ours)	50.04	0.3060	<b>88.51*</b>	<b>0.7429*</b>	<b>53.81*</b>	<b>0.2273*</b>
	$\Delta$	-0.70	-0.0031	-3.51	-0.0293	+1.03	+0.0041
DistMult	Self-Adv.	<b>48.41</b>	<b>0.3091</b>	<b>92.94</b>	<b>0.6837</b>	<b>53.80</b>	<b>0.4399</b>
	Self-Adv. SANS (ours)	<b>48.68*</b>	<b>0.3100*</b>	<b>93.04*</b>	<b>0.7561*</b>	38.70	0.3684
	Self-Adv. RW-SANS (ours)	48.17	0.3071	91.08	0.6634	<b>42.74*</b>	<b>0.3836*</b>
	$\Delta$	+0.27	+0.0009	+0.10	+0.0724	-11.06	-0.0563
RotatE	Self-Adv.	<b>53.03</b>	<b>0.3362</b>	<b>96.05</b>	<b>0.9498</b>	<b>57.29</b>	<b>0.4760</b>
	Self-Adv. SANS (ours)	<b>53.12*</b>	<b>0.3358*</b>	95.85	0.9494	<b>57.12*</b>	0.4745
	Self-Adv. RW-SANS (ours)	51.07	0.3161	<b>96.09*</b>	<b>0.9496*</b>	56.94	<b>0.4805*</b>
	$\Delta$	+0.09	-0.0004	+0.04	-0.0002	-0.17	+0.0045

Table 2: Comparison of the Self-Adversarial negative sampling technique with our Self-Adversarial SANS. **Marked bold\*** numbers are the results of the best SANS implementation.

with TransE, and is the second best-performing algorithm when combined with DistMult without requiring additional parameters. We observe average  $\Delta$  values of 0.0231,  $-0.0341$ , and 0.0056 in MRR for TransE, DisMult, and RotateE respectively, which confirm our approach’s effectiveness compared to SOTA while remaining computationally efficient.

We also qualitatively investigate the semantic hardness of SANS negatives against negatives generated via uniform sampling. For instance, using the center node “arachnoid” in the WN18RR dataset as an example, the negatives sampled via SANS within a 2-hop neighborhood are “arachnida,” “biology,” “arthropod,” “wolf spider,” and “garden spider,” while the ones picked by uniform sampling are “diner,” “refusal,” “landscape,” “rise,” and “nursery.” Clearly, the negatives found via SANS are semantically harder to distinguish,

and as a result, they also confirm the importance of incorporating graph structure into negative samplers to aid in ‘hard’ negative mining. A more detailed qualitative analysis of negative samples—including the effect of varying neighborhood sizes—generated by SANS can be found in C.1.

**Q2:** We now combine our approach SANS with Self-Adversarial negative sampling (Sun et al., 2019). Our results are presented in Table 2 under Self-Adv. SANS and Self-Adv. RW-SANS, both of which reweigh the negative triplets as done in (Sun et al., 2019). We observe comparable performance between the two approaches, but crucially this is achieved by mostly considering 0.2% to 9% of the entities in the datasets like in WN18 and WN18RR, as indicated in Table 3. By considering that the partially-filled adjacency tensors improve computational feasibility for requiring less memory and allowing sparse tensor operations to take place,

the appeal of incorporating graph structure while choosing negative samples is further highlighted.

$k$	2	3	4	5
FB15K-237	34	83	97	99
WN18	0.19	0.75	3.22	10.2
WN18RR	0.16	0.65	2.76	8.67

Table 3: Percentage (%) of filled entries in the  $k$ -hop adjacency tensor.

**Q3:** We now analyze the impact of approximating the local neighborhood using random walks. Fig. 2 depicts the effect of varying the number of random walks ( $\omega$ ) with neighborhoods of different radii and MRR. We report two baselines, one being the performance of uniform sampling, and the other being our best performance achieved by Uniform SANS when combined with TransE, for which the  $k$ -hop tensor was explicitly computed. Interestingly, we find that the  $k$ -hop tensor can not only be well approximated with 3000 random walks, but RW-SANS beats both baselines. We reconcile this result by noting that certain nodes have a higher probability of being sampled due to sharing a larger number of paths with the center node, resulting in an implicit weighted negative sampling scheme.

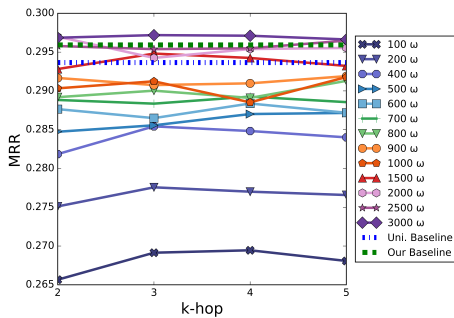


Figure 2: The performance of Uniform RW-SANS with TransE on FB15K-237 using different  $\omega$  values.

## 5 Conclusion and Future Directions

In this work, we introduced SANS, a novel negative sampling strategy, which directly leverages information about  $k$ -hop neighborhoods to select negative examples. Our work sheds light on the need and importance of incorporating graph structure when designing negative samplers for KGs, and for which SANS can be seen as a cheap yet powerful baseline that requires no additional parameters or difficult optimization. Empirically, we find that

SANS-based negatives have comparable performance with SOTA approaches and even outperform previous sophisticated GAN-based approaches.

## Acknowledgments

The authors would like to thank the anonymous EMNLP reviewers for their helpful and constructive feedback. This research was supported by a Canada CIFAR AI Chair and NSERC Discovery Grant RGPIN-2019-0512. Avishek Joey Bose is also generously supported through the IVADO PhD fellowship.

## References

- Gabor Angeli and Christopher D Manning. 2013. Philosophers are mortal: Inferring the truth of unseen facts. In *Proceedings of the seventeenth conference on computational natural language learning*, pages 133–142.
- Yoshua Bengio, Jean-Sébastien Senécal, et al. 2003. Quick training of probabilistic neural nets by importance sampling. In *AISTATS*, pages 1–9.
- Jonathan Berant, Andrew Chou, Roy Frostig, and Percy Liang. 2013. Semantic parsing on freebase from question-answer pairs. In *Proceedings of the 2013 conference on empirical methods in natural language processing*, pages 1533–1544.
- Kurt Bollacker, Colin Evans, Praveen Paritosh, Tim Sturge, and Jamie Taylor. 2008. Freebase: a collaboratively created graph database for structuring human knowledge. In *Proceedings of the 2008 ACM SIGMOD international conference on Management of data*, pages 1247–1250.
- Antoine Bordes, Nicolas Usunier, Alberto Garcia-Duran, Jason Weston, and Oksana Yakhnenko. 2013. Translating embeddings for modeling multi-relational data. In *Advances in neural information processing systems*, pages 2787–2795.
- Avishek Joey Bose, Huan Ling, and Yanshuai Cao. 2018. Adversarial contrastive estimation. In *Proceedings of the 56th Annual Meeting of the Association for Computational Linguistics (Volume 1: Long Papers)*, pages 1021–1032.
- Liwei Cai and William Yang Wang. 2018. Kbgan: Adversarial learning for knowledge graph embeddings. In *Proceedings of the 2018 Conference of the North American Chapter of the Association for Computational Linguistics: Human Language Technologies, Volume 1 (Long Papers)*, pages 1470–1480.
- Ronan Collobert and Jason Weston. 2008. A unified architecture for natural language processing: Deep neural networks with multitask learning. In *Proceedings of the 25th international conference on Machine learning*, pages 160–167.

- Ian Goodfellow, Jean Pouget-Abadie, Mehdi Mirza, Bing Xu, David Warde-Farley, Sherjil Ozair, Aaron Courville, and Yoshua Bengio. 2014. Generative adversarial nets. In *Advances in neural information processing systems*, pages 2672–2680.
- Michael Gutmann and Aapo Hyvärinen. 2010. Noise-contrastive estimation: A new estimation principle for unnormalized statistical models. In *Proceedings of the Thirteenth International Conference on Artificial Intelligence and Statistics*, pages 297–304.
- Yanchao Hao, Yuanzhe Zhang, Kang Liu, Shizhu He, Zhanyi Liu, Hua Wu, and Jun Zhao. 2017. An end-to-end model for question answering over knowledge base with cross-attention combining global knowledge. In *Proceedings of the 55th Annual Meeting of the Association for Computational Linguistics (Volume 1: Long Papers)*, pages 221–231.
- Tomas Mikolov, Ilya Sutskever, Kai Chen, Greg S Corrado, and Jeff Dean. 2013. Distributed representations of words and phrases and their compositionality. In *Advances in neural information processing systems*, pages 3111–3119.
- George A Miller. 1995. Wordnet: a lexical database for english. *Communications of the ACM*, 38(11):39–41.
- Dan I Moldovan and Vasile Rus. 2001. Logic form transformation of wordnet and its applicability to question answering. In *Proceedings of the 39th Annual Meeting on Association for Computational Linguistics*, pages 402–409. Association for Computational Linguistics.
- Bryan Perozzi, Rami Al-Rfou, and Steven Skiena. 2014. Deepwalk: Online learning of social representations. In *Proceedings of the 20th ACM SIGKDD international conference on Knowledge discovery and data mining*, pages 701–710.
- Matthew E Peters, Mark Neumann, Robert Logan, Roy Schwartz, Vidur Joshi, Sameer Singh, and Noah A Smith. 2019. Knowledge enhanced contextual word representations. In *Proceedings of the 2019 Conference on Empirical Methods in Natural Language Processing and the 9th International Joint Conference on Natural Language Processing (EMNLP-IJCNLP)*, pages 43–54.
- Noah A Smith and Jason Eisner. 2005. Contrastive estimation: Training log-linear models on unlabeled data. In *Proceedings of the 43rd Annual Meeting on Association for Computational Linguistics*, pages 354–362. Association for Computational Linguistics.
- Zhiqing Sun, Zhi-Hong Deng, Jian-Yun Nie, and Jian Tang. 2019. Rotate: Knowledge graph embedding by relational rotation in complex space. In *International Conference on Learning Representations*.
- Peifeng Wang, Shuangyin Li, and Rong Pan. 2018. Incorporating gan for negative sampling in knowledge representation learning. In *Thirty-Second AAAI Conference on Artificial Intelligence*.
- Dirk Weissenborn, Pasquale Minervini, Isabelle Augenstein, Johannes Welbl, Tim Rocktäschel, Matko Bosnjak, Jeff Mitchell, Thomas Demeester, Tim Dettmers, Pontus Stenetorp, et al. 2018. Jack the reader—a machine reading framework. In *Proceedings of ACL 2018, System Demonstrations*, pages 25–30.
- Bishan Yang and Tom Mitchell. 2017. Leveraging knowledge bases in lstms for improving machine reading. In *Proceedings of the 55th Annual Meeting of the Association for Computational Linguistics (Volume 1: Long Papers)*, pages 1436–1446.
- Xuchen Yao and Benjamin Van Durme. 2014. Information extraction over structured data: Question answering with freebase. In *Proceedings of the 52nd Annual Meeting of the Association for Computational Linguistics (Volume 1: Long Papers)*, pages 956–966.
- Mo Yu and Mark Dredze. 2014. Improving lexical embeddings with semantic knowledge. In *Proceedings of the 52nd Annual Meeting of the Association for Computational Linguistics (Volume 2: Short Papers)*, pages 545–550.
- Yongqi Zhang, Quanming Yao, Yingxia Shao, and Lei Chen. 2019. Nscaching: Simple and efficient negative sampling for knowledge graph embedding. In *2019 IEEE 35th International Conference on Data Engineering (ICDE)*, pages 614–625. IEEE.

## A Experimental Settings

This section provides an overview of the datasets and evaluation protocols used for obtaining our results.

### A.1 Datasets

To conduct experiments for our proposed methods, datasets FB15K-237, WN18, and WN18RR were used. FB15K-237 is a subset of FB15K, which has been derived from the FreeBase Knowledge Base (KB) (Bollacker et al., 2008), a large database that contains general facts about the world with many different relation types. On the other hand, WN18RR is a subset of WN18, which has been derived from the WordNet KB (Miller, 1995), which is a large lexical English database that captures lexical relations—e.g. the super-subordinate relations between words. The WN18 and FB15K were first introduced in (Bordes et al., 2013) and were used in the majority of KG-related researches. In comparison, WN18 and WN18RR contain less relation

types than FB15K-237. A summary of the number of entities and relation types corresponding to each of these datasets is provided in Table 4.

Dataset	#entity	#relation
FB15K-237	14,541	237
WN18	40,943	18
WN18RR	40,943	11

Table 4: Dataset Information (Sun et al., 2019).

## A.2 Evaluation Protocols

To evaluate our negative sampling approach, we used standard evaluation metrics, consisting of Mean Reciprocal Rank (MRR) and Hits at N (H@N). The train/validation/test split information is provided in Table 5.

Dataset	#training	#validation	#test
FB15K-237	272,115	17,535	20,466
WN18	141,442	5,000	5,000
WN18RR	86,835	3,034	3,134

Table 5: Train/Validation/Test Split Information (Sun et al., 2019).

## B Implementation Details

This section of the supplemental goes over the implementation details of our RW-SANS algorithms—i.e. Uniform RW-SANS and Self-Adv. RW-SANS, which use random walks to approximate the  $k$ -hop adjacency tensor. Other experimental setups are further detailed herein.

### B.1 Hyperparameters

$k$  and  $\omega$  (for when the  $k$ -hop neighborhood is being approximated by Alg. 1) are the hyperparameters in our negative sampling algorithms. To find the optimal hyperparameter values that resulted in the highest performance on the validation set of different datasets,  $k$  and  $\omega$  values in range 2 to 8 and 1000 to 5000 were used respectively during the negative sampling step. In other words, the best performances on the validation sets in our empirical study were found by manual tuning of the hyperparameters. More information about the experimental trials can be found in Table 6, where the total number of trials for training each of the graph embedding models on each dataset is also indicated.

SANS Algorithm	$k$ -range	$\omega$ -set	#trials
Uniform/ Self-Adv	2-8	N/A	7
Uniform RW/ Self-Adv RW	2-5	{1000, 1500, ..., 4500}	32

Table 6: Hyperparameter combination sets and number of trials per model.

Additionally, Table 7 lists the hyperparameters with which different graph embedding models were trained to reach their optimal performance on the validation sets.

Hyper-parameter	TransE	DistMult	RotatE
Embedding Dimension	1024	1024	1024
Batch Size	1000	2000	1000
$\gamma$	9	200	9
Optimizer	Adam	Adam	Adam
$\alpha$	5E-05	1E-03	5E-05

Table 7: Graph Embedding Models’ Hyperparameters.

### B.2 Preprocessing

Building the  $k$ -hop neighborhood of the nodes within the KG can be regarded as the preprocessing step, essential to implementing SANS. In this paper, we propose two techniques for doing so, which are:

1. explicit computation of the  $k$ -hop neighborhood by manipulating Eqn. 2 while accounting for different relation types and,
2. approximation of the  $k$ -hop neighborhood using random walks, as detailed in Alg. 1.

### B.3 Infrastructure Settings

The experiments in our study were carried on a server with one NVIDIA V100 GPU, 10 CPU cores, and 46GB RAM.

## C Experimental Results

### C.1 Qualitative Assessment of Negative Samples

In this section, we assess the semantic meaningfulness of negative samples produced by Uniform SANS and those produced by uniform sampling using the WN18RR dataset. As presented by the

Anchor Node	Candidate Nodes				
	Uniform	$k = 2$	$k = 3$	$k = 4$	$k = 5$
arachnoid	diner	arachnida	biological	plectognathi	actinidia
	refusal	biology	ostracoda	neritidae	bangiaceae
	landscape	arthropod	subkingdom	amphibian_family	barn_spider
	rise	wolf spider	placodermi	pelecaniformes	holarrhena
empathy	nurser	garden spider	scyphozoa	categorize	lucilia
	beach pea	sympathetic	sympathizer	cheerlessness	cheerfulness
	sanvitalia	sympathy	expectation	ambition	pleasure
	albinism	feeling	passion	have a bun in the oven	sympathize
wheat	micromeria	commiserate	pride	pleasure	enjoyment
	banking industry	commiseration	state	attribute	stimulate
	lend	wild rice	fast food	Edirne	Jena
	align	tabbouleh	salad	United States	seasoning
wheat	doodad	barley	mess	fixings	Washington
	mismanage	Bulgur	stodge	form	pudding
	semiconductor device	buckwheat	meal	Iraqi Kurdistan	Bursa

Table 8: Example set of candidate nodes to form a negative triplet given an anchor node produced by uniform sampling (Uniform) and Uniform SANS. In this table,  $k$  refers to the radius of the  $k$ -hop neighbourhood from which the candidate nodes are drawn by SANS.

Dataset	Score Function	SANS Algorithm	$k$	H@10		MRR	
				Validation	Test	Validation	Test
FB15K-237	TransE	Uniform	3	48.55	48.35	0.3010	0.2962
		Self-Adversarial	3	52.51	52.03	0.3340	0.3265
	DistMult	Uniform	3	40.86	41.00	0.2599	0.2595
		Self-Adversarial	3	49.07	48.68	0.3131	0.3100
	RotatE	Uniform	3	48.64	48.22	0.3031	0.2985
		Self-Adversarial	5	53.72	53.12	0.3432	0.3358
WN18	TransE	Uniform	5	94.97	95.09	0.8237	0.8228
		Self-Adversarial	5	84.61	84.06	0.7165	0.7136
	DistMult	Uniform	3	93.07	93.19	0.7507	0.7553
		Self-Adversarial	3	92.90	93.04	0.7534	0.7561
	RotatE	Uniform	4	95.69	95.97	0.9492	0.9499
		Self-Adversarial	5	95.61	95.85	0.9489	0.9494
WN18RR	TransE	Uniform	4	50.89	51.15	0.2228	0.2254
		Self-Adversarial	8	52.46	53.21	0.2207	0.2249
	DistMult	Uniform	6	44.73	44.74	0.4047	0.4025
		Self-Adversarial	8	39.01	38.70	0.3749	0.3684
	RotatE	Uniform	4	55.78	55.76	0.4816	0.4769
		Self-Adversarial	8	56.76	57.12	0.4788	0.4745

Table 9: The hyperparameter values associated with the best performance on the validation sets, used for obtaining the test results. The different variations of SANS in this table explicitly compute the  $k$ -hop adjacency tensor.

examples given in Table 8, Uniform SANS results in negative examples that are harder to distinguish semantically compared to uniform sampling. We also notice the semantic meaningfulness of SANS-based negatives decline as we increase the size of the  $k$ -hop neighbourhood. This observation is indeed expected since as the neighbourhood increases in size (i.e.  $k \rightarrow \infty$ ) Uniform SANS will become analogous to uniform sampling.

## C.2 SOTA Algorithms

Results for the Uniform and Self-Adversarial algorithms in Table 1 and Table 2 respectively were achieved by re-running the code provided by (Sun et al., 2019) using the hyperparameters they re-

ported for the best performance on the validation set of different datasets. Additionally, the results for KBGAN and NSCaching in Table 1 are the *scratch* results directly taken from (Zhang et al., 2019).

## C.3 SANS Algorithms

Table 9 and Table 10 report the performance of the graph embedding models fused with our negative sampling techniques on the validation and test sets with respect to the evaluation metrics. Additionally, they list the hyperparameter values corresponding to Uniform/Self-Adv. SANS and Uniform/Self-Adv. RW-SANS that resulted in the best performance on the validation sets. Based on our out-



Dataset	Score Function	SANS Algorithm	$k$	$\omega$	H@10		MRR	
					Validation	Test	Validation	Test
FB15K-237	TransE	Uniform	5	4000	49.12	48.50	0.3023	0.2981
		Self-Adversarial	4	4000	50.59	50.04	0.3129	0.3060
	DistMult	Uniform	4	3000	41.66	41.46	0.2628	0.2621
		Self-Adversarial	5	3000	48.67	48.17	0.3142	0.3071
	RotatE	Uniform	2	4000	49.05	48.47	0.3034	0.3003
		Self-Adversarial	2	4000	51.41	51.07	0.3205	0.3161
WN18	TransE	Uniform	2	1000	95.23	95.22	0.8194	0.8195
		Self-Adversarial	3	4000	88.65	88.51	0.7480	0.7429
	DistMult	Uniform	2	1000	89.38	89.80	0.6205	0.6235
		Self-Adversarial	2	1000	90.55	91.08	0.6601	0.6634
	RotatE	Uniform	2	3000	95.92	96.07	0.9492	0.9489
		Self-Adversarial	2	4500	95.83	96.09	0.9493	0.9496
WN18RR	TransE	Uniform	2	1000	52.67	53.41	0.2282	0.2317
		Self-Adversarial	5	2000	53.05	53.81	0.2229	0.2273
	DistMult	Uniform	2	3000	49.01	49.09	0.4111	0.4071
		Self-Adversarial	4	1000	43.70	42.74	0.3883	0.3836
	RotatE	Uniform	2	1000	57.20	57.12	0.4860	0.4796
		Self-Adversarial	2	1000	57.09	56.94	0.4882	0.4805

Table 10: The hyperparameter values associated with the best performance on the validation sets, used for obtaining the test results. The different variations of SANS in this table approximate the  $k$ -hop adjacency tensor by random walks (RW-SANS) using Alg. 1.

Negative Sampling Algorithm	Preprocessing Complexity	Runtime Complexity	Space Complexity
Uniform (Bordes et al., 2013)	$O(1)$	$O(bn)$	$O(1)$
KBGAN (Cai and Wang, 2018)	$O(t)$	$O(bn + bd + bt)$	$O(t)$
NSCaching (Zhang et al., 2019)	$O(1)$	$O(bn + be)$	$O(c R  V )$
Self-Adv. (Sun et al., 2019)	$O( E )$	$O(bn + bd)$	$O( E )$
Uniform SANS (ours)	$O( V ^3 \log k)$	$O(bn)$	$O( V ^2)$
Self-Adv. SANS (ours)	$O( V ^3 \log k)$	$O(bn + bd)$	$O( V ^2)$
Uniform RW-SANS (ours)	$O(rk V )$	$O(bn)$	$O(r V )$
Self-Adv. RW-SANS (ours)	$O(rk V )$	$O(bn + bd)$	$O(r V )$

Table 11: Comparison of different negative sampling algorithms in terms of preprocessing, runtime, and space complexities given batch size  $b$ , negative sample size  $n$ , cache size  $c$ , cache extension size  $e$ , node set  $V$ , edge set  $E$ , relation set  $R$ , embedding dimension  $d$ , hops count  $k$ , random walks count  $r$ , and GAN parameters count  $t$ .

comes, we hypothesize that the usage of random walks in approximating the  $k$ -hop neighborhood implicitly results in the removal of nodes with the least number of walks to the center node—i.e. outlier nodes.

## D Computational Complexity

Table 11 is representative of the time and space complexities of different negative sampling approaches including SANS.